Mathematical Model of Heat Flow and Austenite-Pearlite Transformation in Eutectoid Carbon Steel Rods for Wire

PRAKASH K. AGARWAL AND J. K. BRIMACOMBE

A mathematical model incorporating both heat transfer and the transformation of austenite to pearlite in eutectoid carbon steel rods has been developed. A computer program based on the implicit finite-difference technique has been written which permits the temperature distribution and fraction of austenite transformed to be predicted as a function of cooling conditions, rod diameter and the transformation characteristics of the steel. The program takes into account the temperature-dependent heat transfer and thermophysical properties; and stresses the importance of the enthalpy of transformation. The model has been checked for internal consistency with theoretical equations, and model predictions have been compared to published industrial data for rod cooling in water at 100 °C. The effect on the temperature distribution and fraction of austenite transformed of several variables, *viz.*, rod diameter, starting temperature, heat transfer conditions, transformation characteristics and quenchant temperature, has been predicted using the model. The range of variables studied are typical of those found in industrial processes such as patenting and controlled cooling. Use of the model in the design of controlled cooling processes and in coping with problems such as segregation in wire rods is currently under study.

THE prediction of phase transformations in metal heat-treatment processes, such as the controlled cooling of wire rod, is made difficult by the complex nature of the coupled heat transfer and phase-transformation kinetics. Heat transfer at the surface of the metal, for example, depends on local cooling conditions which change with temperature, fluid properties and relative fluid velocity. Likewise within the metal, the thermophysical properties vary with temperature; and heat due to the transformation is evolved. Also the transformation kinetics depend on cooling rate, steel composition and austenite grain size, and have been inadequately characterized, from the processing standpoint, in terms of isothermal or constant cooling conditions, which do not obtain in real processes. For these reasons the mathematical modelling of heat-treatment processes has not developed to the same extent as in other processes like continuous casting.

The need to develop such models, however, is clear since then design of the processes can be based on first principles with less guesswork involved, and the solution to problems such as those arising from macrosegregation achieved rapidly and rationally. Thus in the present work, a mathematical model has been formulated which incorporates the important physical phenomena in the heat treatment of eutectoid carbon steel rods. In the present paper, the validity of the model is tested against limited experimental measurements reported in the literature; and the influence of variables, *viz* rod diameter, cooling conditions, finishing temperature and steel composition, on the temperature field, and austenite-pearlite transformation is predicted. In subsequent papers a rigorous evaluation of the model, employing temperature and transformation data measured in our laboratory, will be presented together with examples of the use of the model in the analysis, improvement and design of controlled cooling processes such as Stelmor.

PRAKASH K. AGARWAL, formerly Graduate Student in the Department of Metallurgical Engineering, University of British Columbia, is now with IVACO, L'Orignal, Ontario. J. K. BRIMACOMBE is Stelco Professor of Process Metallurgy, Department of Metallurgical Engineering, University of British Columbia, Vancouver, B. C. V6T IW5, Canada.

Manuscript submitted March 17, 1980.

1. MATHEMATICAL MODEL

The model has been formulated for the case of an infinitely long steel rod moving at high speed through a cooling system or alternatively, for a rod subjected to uniform cooling over its length. In both cases axial heat conduction can be ignored, in the former because it is negligible compared to the bulk flow of heat, and in the latter because axial temperature gradients are small. The following assumptions have also been made in the formulation:

i) uniform initial temperature
ii) radial symmetry
iii) temperature independent of angular displacement
iv) uniform circular cross-section

Under these conditions, heat flow within the rod is governed by the following equation:

$$\frac{\partial}{\partial r}\left(k\frac{\partial T}{\partial r}\right)+\frac{k}{r}\frac{\partial T}{\partial r}+\dot{q}_{AP}=\rho C_p\frac{\partial T}{\partial t} \qquad [1]$$

Note that $\dot{q}_{AP}$ is the volumetric rate of heat generation within the rod due to the austenite-pearlite transformation. The following boundary conditions have been applied:

i) at the centerline

$$t>0,\quad r=0,\quad -k\frac{\partial T}{\partial r}=0 \qquad [2]$$

ii) at the rod surface

ISSN 0360-2141/81/0311-0121$00.75/0

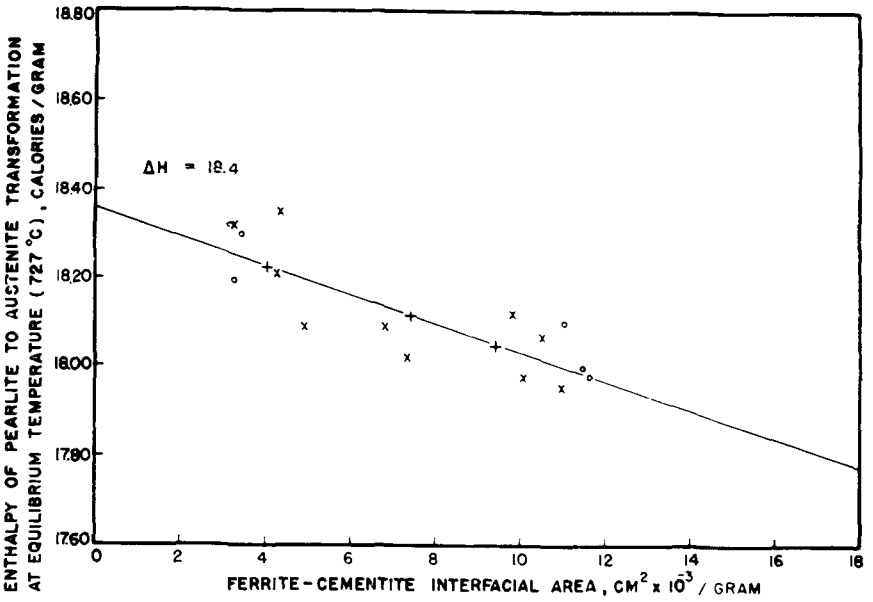

Fig. 1—Influence of ferrite-cementite interfacial area on enthalpy of pearlite to austenite transformation (after Kramer *et al*).

$$t > 0, \quad r = r_o, \quad -k\frac{\partial T}{\partial r} = h(T_{r_o} - T_a) \qquad [3]$$

while the initial condition is

$$t = 0, \quad 0 \leqslant r \leqslant r_o, \quad T = T_{in} \qquad [4]$$

In the model k and C_P have been taken to be linear functions of temperature and are based on the fraction of austenite and pearlite present using the BISRA data.[1] On the other hand, ρ has been assumed constant.

The enthalpy of the austenite to pearlite transformation has a value of 75.8 kJ/kg at the $A\,C_1$ temperature, according to Kramer *et al*[2] for eutectoid carbon steel. The influence of specific ferrite-cementite interfacial area (proportional to pearlite spacing) on the transformation enthalpy has been neglected because, as shown in Fig. 1, the effect is small. Similarly the effect of strain energy associated with the volume change due to transformation has been ignored. However, the influence of temperature on the transformation enthalpy has been included in the model using the specific heats of austenite and pearlite which, when necessary, have been obtained by extrapolation.

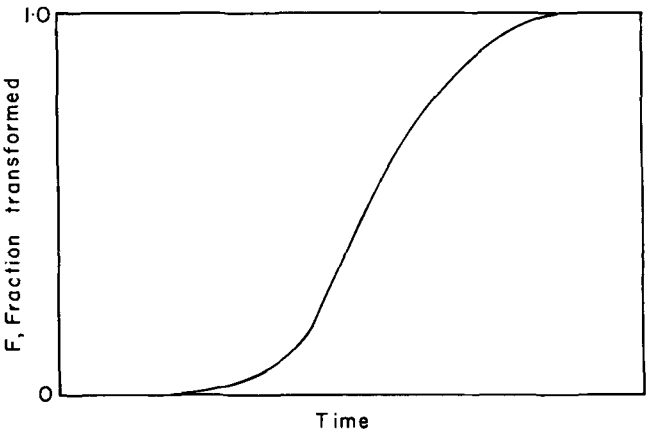

Fig. 2—General curve for fraction austenite transformed vs time at constant temperature.

The heat-transfer coefficient appearing in Eq. [3] has been specified in the model as either a constant value or a function of temperature and fluid flow conditions. The constant h has been used when only approximate values are available. The variable h has been employed in systems where radiation predominates or fluid flow is reasonably well defined so that heat-transfer correlations[3] can be applied. An example is the Stelmor process[4] in which air is blown over the wire rod. An alternative to Eq. [3] for the surface boundary condition is the specification of surface temperature. This can be used when the model is applied to design calculations where theoretical values of surface heat flux are desired.

The austenite-pearlite transformation within the rod has been characterized by the following two-parameter equation

$$F = 1 - \exp[-C(T)\theta^{n(T)}] \qquad [5]$$

where $C(T)$ and $n(T)$ are parameters that vary with temperature, steel composition and austenite grain size. Equation [5] conforms to the generalized curve for the transformation at constant temperature which is shown in Fig. 2. It is readily recognized that Eq. [5] has the same form as the equation originally derived by Johnson and Mehl[5] where $C(T) = (\pi/3)N_v G^3$ and $n = 4$. Their equation was based on numerous assumptions which included random nucleation and growth, and constant nucleation rate. However it is unlikely that these conditions strictly obtain in the steels under study. Hence in the present work, the form of Eq. [5] is assumed to be roughly correct from an empirical standpoint, and the values of $C(T)$ and $n(T)$ have been determined at each temperature from the "start" and "end" isotransformation C-curves on the appropriate T-T-T diagram.[6,7] These curves correspond to 0.1 pct[7] and 99.9 pct (assumed) transformation respectively, subject to the condition that above 723 °C ($A\,C_1$), $F = 0$. The C-curves were approximated by a series of connected semilogarithmic line segments to facilitate the calculation of $C(T)$ and $n(T)$ in the computer program, Fig. 3.

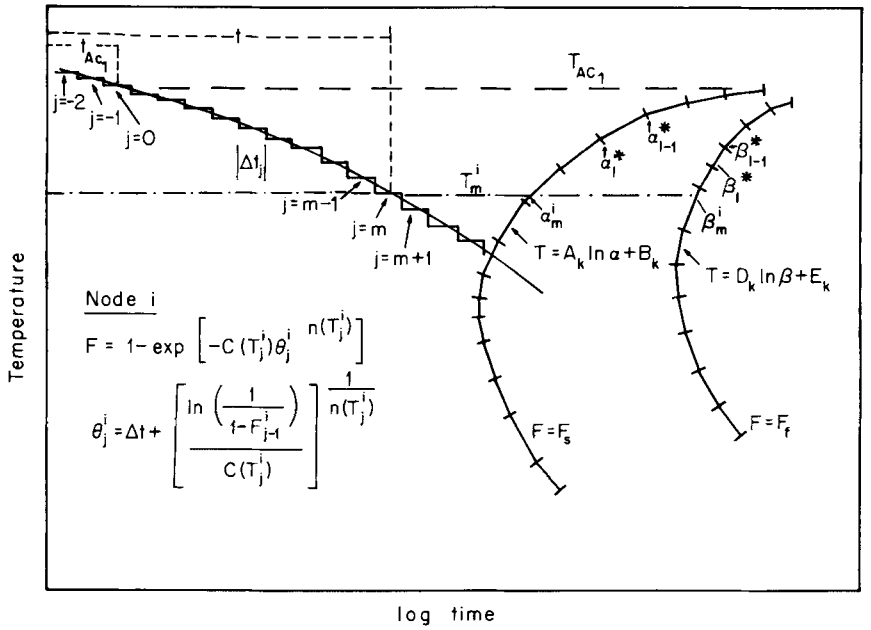

Fig. 3—Subdivision of cooling curve superimposed on a *T-T-T* diagram.

Equation [1] was solved numerically by subdividing time and space into discrete intervals, Δt and Δr respectively, and by applying the implicit finite-difference method. Owing to the dependence of $\dot{q}_{AP}$ on F

$$\dot{q}_{AP} = \rho H (T)_{AP} \frac{\Delta F_{AP}}{\Delta t} \qquad [6]$$

an iterative scheme was required at each time step. Referring to Fig. 3 the fraction of austenite transformed in a given node, i, in each iteration, ΔF_i was calculated in the following way. Commencing with $F = 0$ at the AC_1 temperature, the values of $C(T_o^i)$ and $n(T_o^i)$* were determined for each nodal temperature from the start and end isotransformation curves. Then, assuming isothermal conditions for the duration of the small time interval, typically 0.1 s, Eq. [5] was used to compute F_o^i $(= \Delta F^i)$ for each node. Next the values of $\dot{q}_{AP}^i$ were calculated employing Eq. [6]; Eq. [1] was then re-solved, and the determination of $C(T_o^i)$, $n(T_o^i)$, F_o^i, $\dot{q}_{AP}^i$ and T_o^i repeated iteratively.

* Note: Subscript o denotes time step during which transformation starts.

In the next and succeeding time intervals, Eq. [1] was solved for the approximate temperature distribution using values of k^i, C_p^i and F^i based on temperatures from the previous time step. Then a new fraction transformed, F_j^i for the jth time step, was calculated employing Eq. [5] where the isothermal transformation time, θ_j^i, was taken to be the sum of Δt and the time to achieve the previous fraction transformed, F_{j-1}^i but at the new nodal temperature, T_j^i.

$$\theta_j^i = \Delta t + \left\{\frac{\ln\left[\frac{1}{1 - F_{j-1}^i}\right]}{C(T_j^i)}\right\}^{1/n(T_j^i)} \qquad [7]$$

The fraction transformed over the time interval, ΔF^i, is then $F_j^i - F_{j-1}^i$. Again, the $\dot{q}_{AP}^i$ were calculated according to Eq. [6] and the overall computation of temperatures and fraction transformed, including θ_j^i, repeated iteratively. It should be emphasized that θ_j^i obtained from Eq. [7] are virtual times and bear no relationship to real process time, but are simply the times required to achieve a given fraction of austenite transformed under isothermal conditions in the respective nodes. Finally it may be noted that the temperature dependence of the thermal conductivity has been incorporated by averaging k between adjacent nodes.

The treatment of transformation kinetics described here is similar in some respects to earlier attempts to predict the start of transformation under continuous cooling conditions from *T-T-T* diagrams. Scheil,[8] for example, subdivided the cooling curve into a number of small time steps, Δt_j as shown in Fig. 3, and calculated the fraction of the incubation period (pretransformation) consumed in each step, $\Delta t_j/\alpha_j$. Then, the "start" of transformation occurs when the following condition is fulfilled.

$$\sum_{j=1} \frac{\Delta t_j}{\alpha_j} = 1 \qquad [8]$$

This approach has been adopted in several research studies,[9,10] but it cannot be used to predict the course of transformation during cooling. In Appendix I, the present method is shown to be in accord with the Scheil equation when n in Eq. [5] is constant.

Solution of the tridiagonal matrix resulting from the implicit finite-difference method was achieved using Gaussian elimination.[11] The iteration scheme was found to converge very rapidly so that within about five iterations, successive approximations of temperature differed by less than 10^{-4} °C. An Amdahl 470/V6-II computer and double precision were employed in all calculations. A simplified flow chart for the model is shown in Fig. 4.

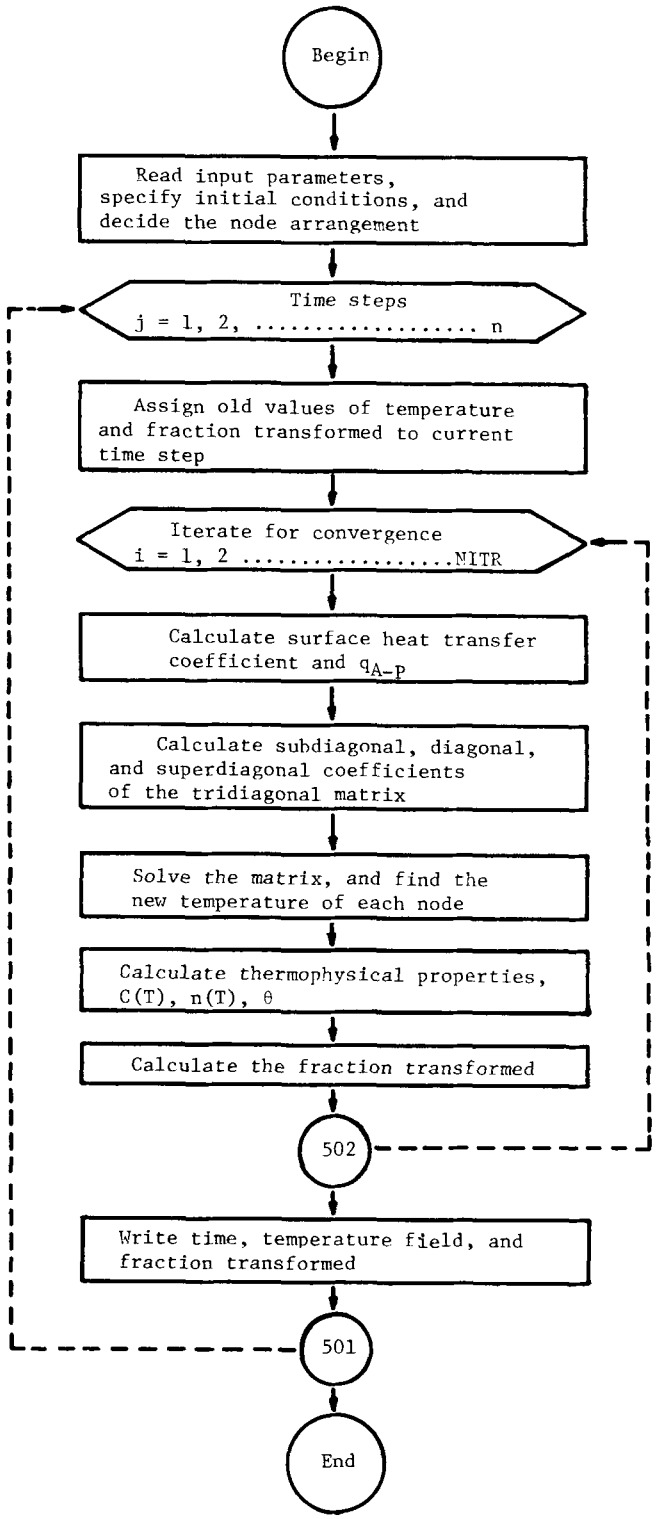

Fig. 4—Flow chart of the computer model.

2. INTERNAL CONSISTENCY CHECKS

The computer model was checked for programming and logic errors in two ways. First, a comparison was made between an analytical solution[12] of Eq. [1], with $\dot{q}_{AP} = 0$ and constant thermophysical properties, and the numerical solution. A comparison was also made for the case of small diameter rods in which the internal resistance to heat flow was negligible.[4] In both situations the model-predicted temperatures were within 1 pct of the analytical values initially, and within 0.1 pct in subsequent calculations.

The second check was made on the phase-transformation section of the model by comparing model predictions of the fraction of austenite transformed to values calculated from Eq. [A18] shown in Appendix II. Equation [A18] was derived for conditions of constant cooling rate, n and Δt. Again, the model-predicted and analytical values of fraction transformed differed by less than 1 pct.

3. MODEL VERIFICATION

The model was next checked against experimental centerline temperatures reported by Takeo *et al*[13] for different sizes of eutectoid carbon steel rods (0.84 pct C, and 0.68 pct Mn) austenitized at 900 °C and quenched in water at 100 °C. The austenite grain size was not given, but is believed to be about 8 to 9 on the ASTM scale. Unfortunately the only *T-T-T* diagram available that matched the composition of the experimental rods corresponded to a larger grain size of 6. Nonetheless it was used in the model predictions together with a heat transfer coefficient of 0.25 kW/m² °C which was derived from other temperature measurements made by these workers using silver rods. Fig. 5 shows a comparison of the predicted and measured center temperatures in four steel rods with different diameters. It is seen that both before and after the transformation, which is characterized by the thermal arrest, the model-predicted temperatures are in reasonable agreement with measured values. However during transformation, the model is under-predicting the temperature by about 35 °C. This indicates that the rate of release of transformation enthalpy which is proportional to the transformation rate is lower in the model than in reality. This dis-

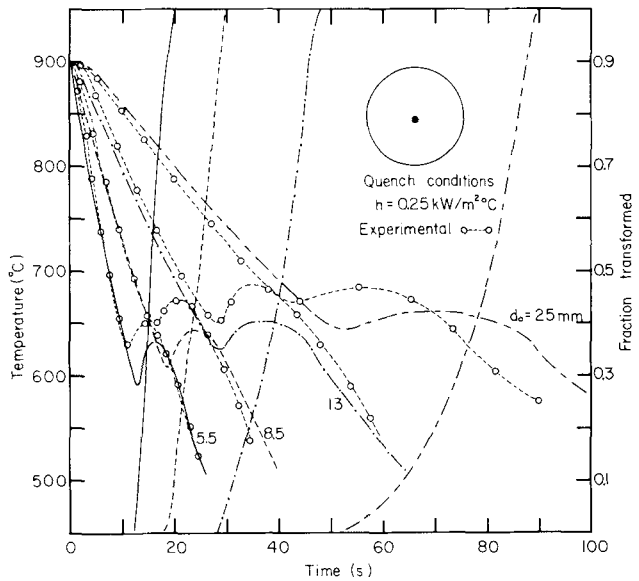

Fig. 5—Comparison of model-predicted temperature to measured temperature in the center of eutectoid carbon steel rods of different diameters.

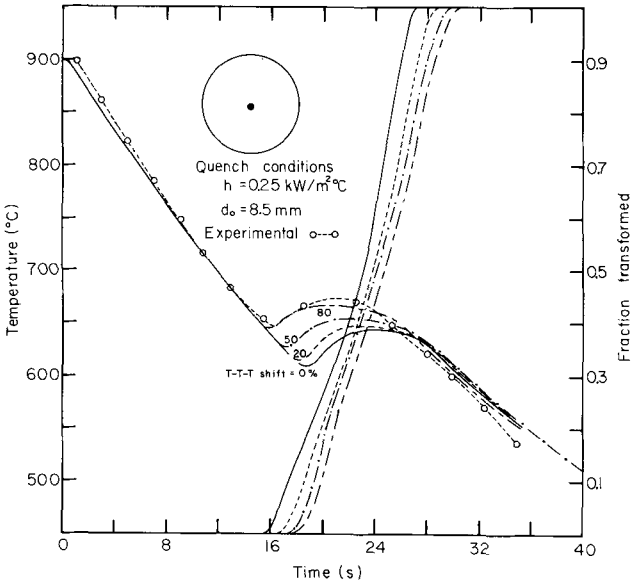

Fig. 6—Effect of shifting the "start" and "end" transformation curves on the predicted center temperature in an 8.5 mm diam rod.

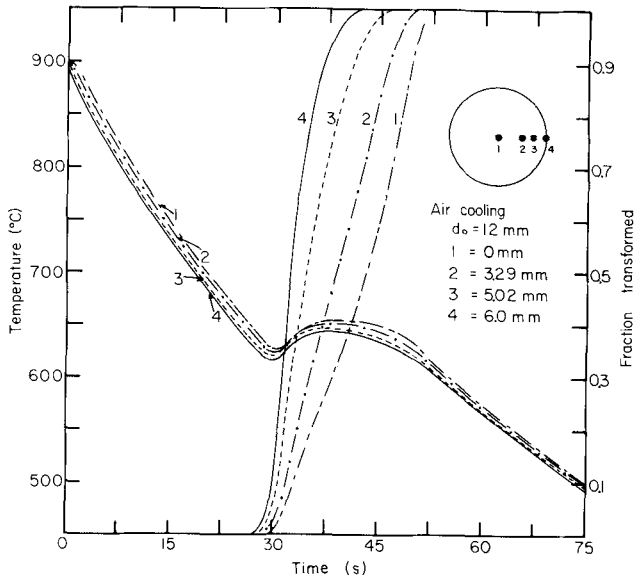

Fig. 8—Predicted temperature and fraction austenite transformed as a function of time at four locations in an air-cooled, 12 mm diam rod.

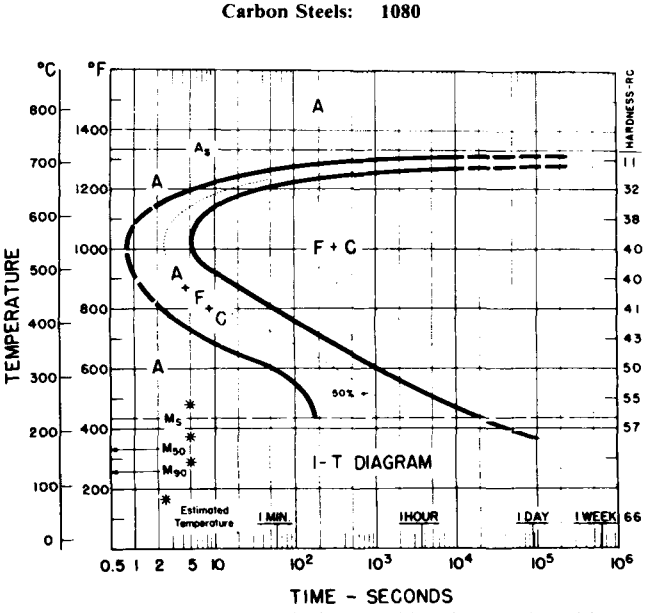

Fig. 7—*T-T-T* diagram for typical eutectoid carbon steel used in majority of calculations. C-0.79; Mn-0.76; austenized at 1650 °F; grain size: 6.

crepancy can easily be explained by the difference in austenite grain size between the experimental rods and the assumed *T-T-T* diagram. The finer grain size in the rods will result in an earlier transformation "start" and a greater transformation rate due to the presence of a larger number of grain boundaries. In other words, the *C*-curves on the assumed *T-T-T* diagram should be shifted to shorter times to accurately represent the experimental rods. The effect of shifting the *C*-curves arbitrarily by 20, 50 and 80 pct is shown in Fig. 6. Thus it is apparent that the shift pushes the temperature up during transformation, and to shorter times, to give a relatively close fit with the experimental curve. Although this does not verify the treatment of phase transformations in the model, it is an encouraging result. Experiments are currently underway in our laboratory to further check this aspect of the model, and will be reported in a following paper.

4. MODEL PREDICTIONS

The model was employed to study the effect of process variables on the temperature and austenite transformation in eutectoid, carbon steel wire rods. The

Table I. Value of Operating Variables Studied

Cooling Method	Variable Studied	Other Variables	Figure
Quench in boiling water	h = 0.25, 0.33, 0.42 kW/m² °C	d_o = 8.5 mm	9
	d_o = 5.5, 8.5, 13.5, 25 mm	h = 0.25 kW/m² °C	10
	Pct Mn = 0.68, 0.87, 1.13, 1.88 (grain size = 5–9)	d_o = 8.5 mm h = 0.25 kW/m² °C	12
Air cool	U_a = 0, 3, 10, 20, 40 m/s	d_o = 5.5 mm	13
	d_o = 5.5, 8.5, 12.0 mm	U_a = 20 m/s	14
	Pct Mn = 0.68, 0.87, 1.13, 1.88 (grain size = 5–9)	d_o = 5.5 mm U_a = 20 m/s	15
	T_{in} = 750,900, 1050 °C	d_o = 5.5 mm U_a = 20 m/s	16
Lead bath	T_{Pb} = 500, 525, 550 °C	d_o = 5.5 mm h = 3.3 kW/m² °C	17

values of variables employed are presented in Table I while the *T-T-T* diagram used for all but four of the cases (pertaining to the effect of pct Mn) is given in Fig. 7.

Figure 8 shows a typical model prediction of the temperature and fraction austenite transformed vs. time at four locations within a 12 mm diam rod cooled with 20 m/s air. In this example the temperature difference between the center and surface of the rod is relatively small, *i.e.* small Biot modulus, particularly before and after the transformation. However, the local transformation at a given time is seen to vary widely through the rod and ultimately the center takes almost 10 s longer than the surface to transform. This of course is due to the transformation thermal arrest which commences at the surface. Thus by first raising the temperature in the outer regions of the rod, the heat of transformation reduces heat extraction from the center of the rod so that the center transformation is retarded and the temperature difference between center and surface is momentarily reduced (~31 s). Shortly thereafter, transformation at the surface is virtually completed, the surface temperature then begins to decrease and heat conduction from the rod interior increases. This permits an increase in the rate of transformation in the center of the rod, and holds the center temperature constant (note the increase in slope of the center transformation curve) until transformation is complete.

Two other aspects of the predictions are of interest from the standpoint of wire-rod production. The first is the time required, from the start of cooling, to complete transformation since this affects the design and operation of the cooling process. The second is the range of the transformation temperature which influences the microstructure of the resultant pearlite; a lower tem-

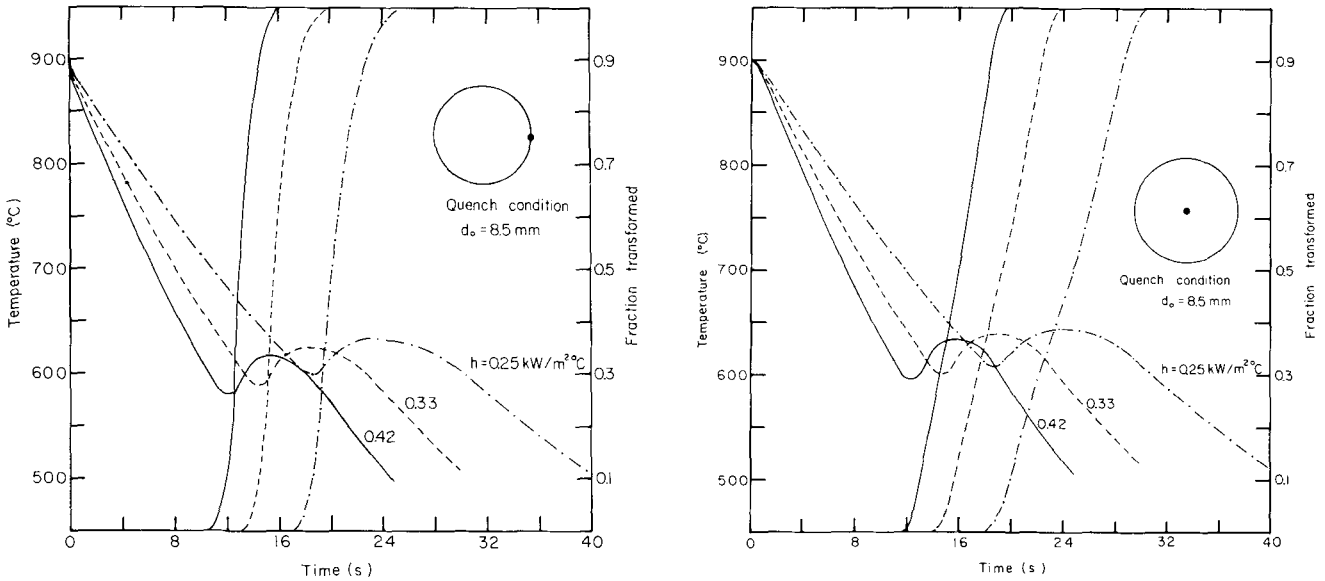

Fig. 9—Effect of heat transfer coefficient on the local temperature and fraction austenite transformed at the surface and center of an 8.5 mm diam rod under quench conditions.

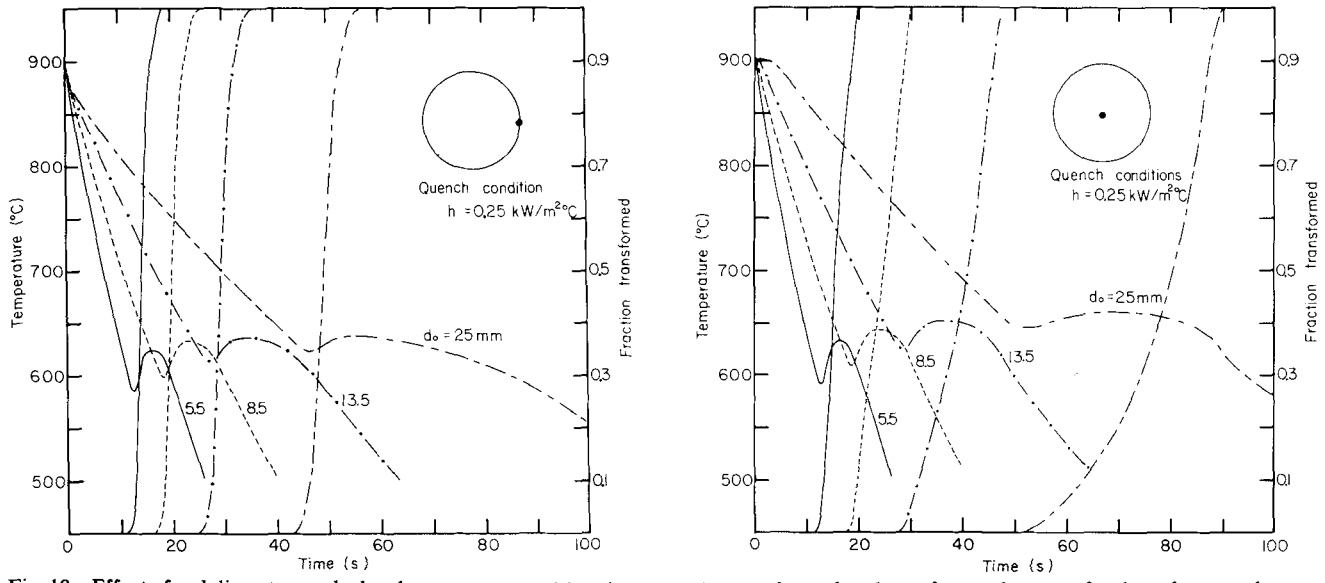

Fig. 10—Effect of rod diameter on the local temperature and fraction austenite transformed at the surface and center of rods under quench conditions.

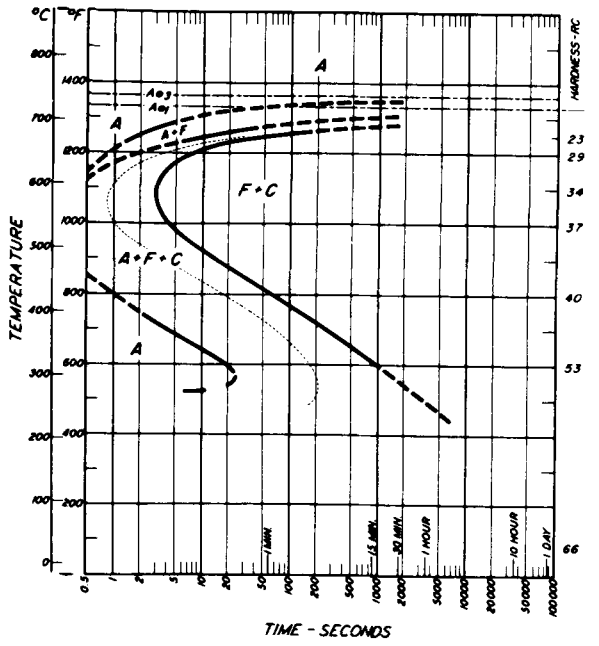

0.64% CARBON STEEL

C - 0.64
Mn - 0.68
Si - 0.22

Austenitizing Temperature : 1600°F.
Grain Size : 6-9

Carbon Steels: 1060

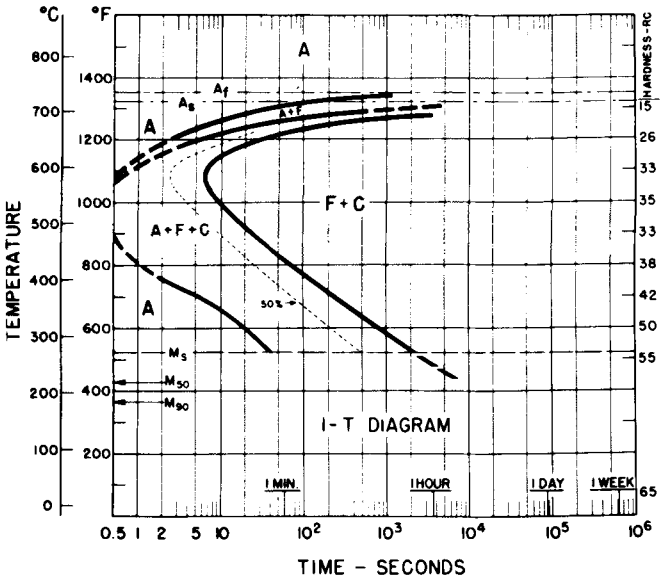

1060

C-0.63
Mn-0.87

Austenitized at 1500°F

Grain Size: 5-6

Carbon Steels: 1566

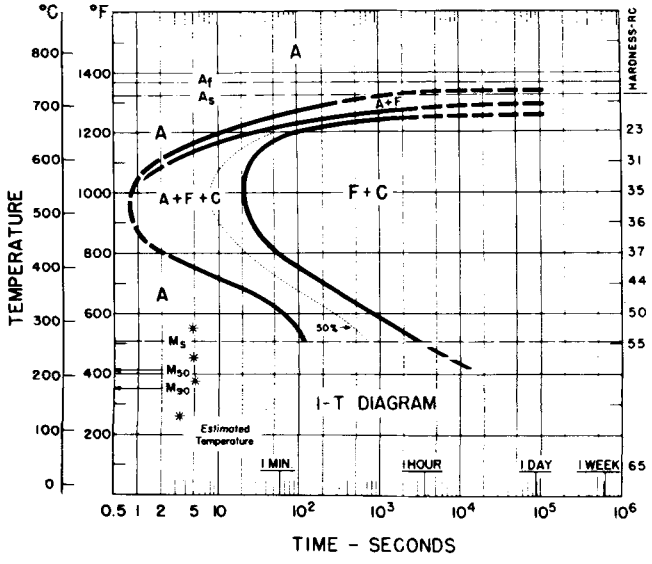

C-0.64
Mn-1.13

Austenitized at 1670°F

Grain Size: 7

Manganese Steels: 1320 Carburized to 0.6C

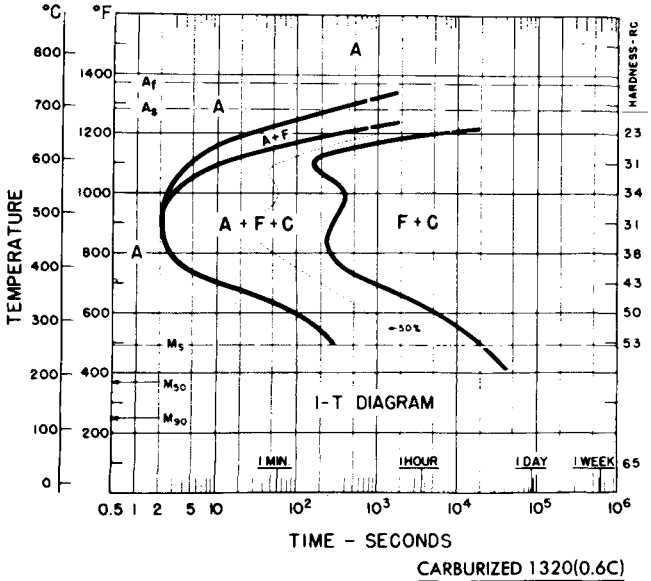

CARBURIZED 1320(0.6C)

C-0.6
Mn-1.88

Austenitized at 1700°F

Grain Size: 5-8
(Occasional 2)

Fig. 11—Isothermal transformation diagrams for four steels exhibiting different pct Mn and grain size.

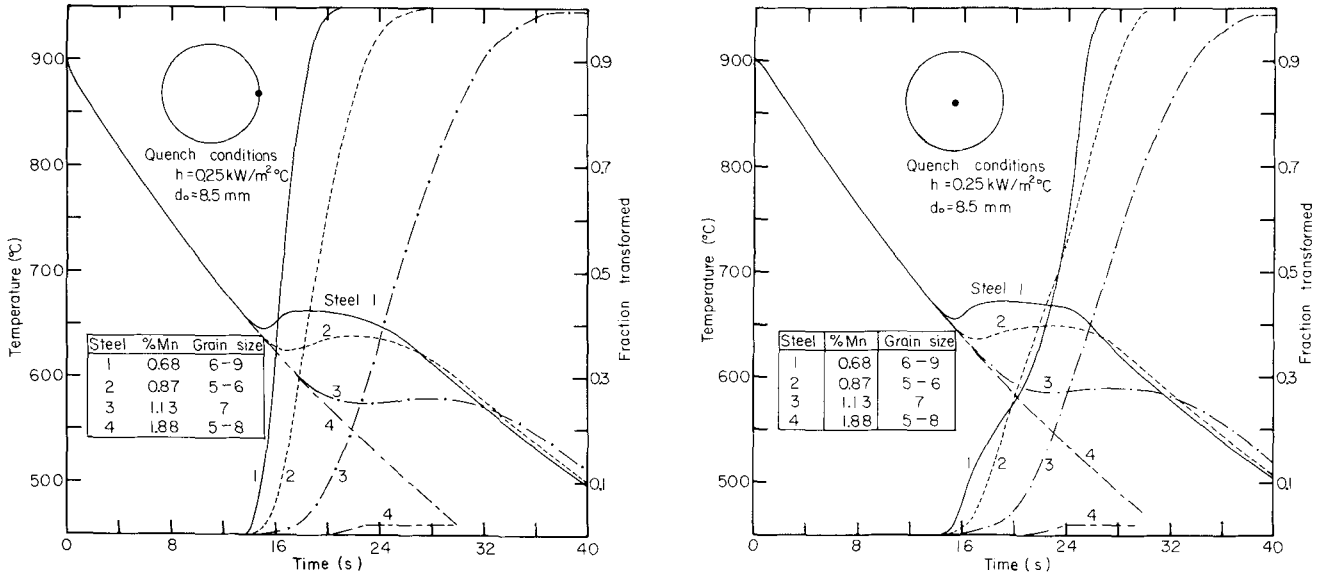

Fig. 12—Effect of pct Mn of steel on the local temperature and fraction austenite transformed at the surface and center of an 8.5 mm diam rod under quench conditions.

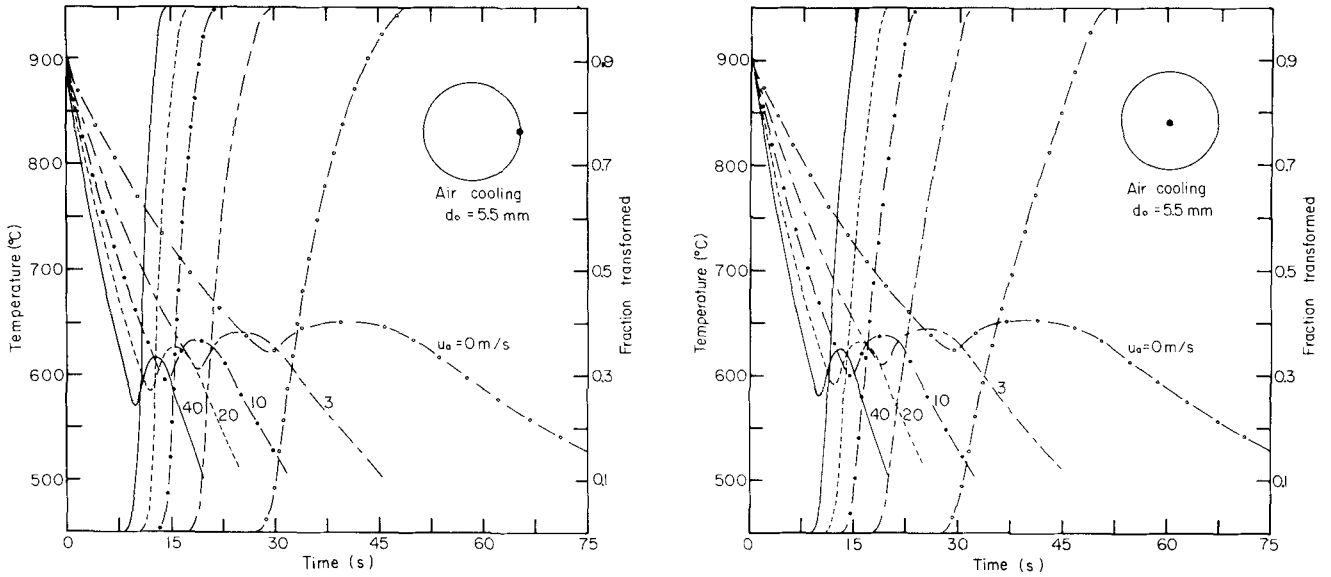

Fig. 13—Effect of air velocity on the local temperature and fraction austenite transformed at the surface and center of a 5.5 mm diam rod.

perature or greater subcooling below T_{AC_1} results in finer pearlite which is desirable for subsequent wire drawing operations. These aspects are discussed briefly in connection with model predictions for three types of cooling.

a. Quench Cooling

This type of cooling has been simulated by using a value of 0.25 kW/m² °C for h in Eq. [3]. This has been derived from the measured temperature response of silver rods, quenched in water at about 95 °C[13] with a correction made for the higher emissivity of steel. The value has been assumed constant since film boiling should prevail throughout the transformation. The effect of increasing h to 0.42 kW/m² °C, which would correspond roughly to quenching in water at 60 °C,[13] is shown in Fig. 9 for an 8.5 mm diam rod. Not unexpectedly, the larger h increases the difference between surface and center temperatures during transformation and also the difference in pearlite spacing through the rod. Increasing h also decreases the range of transformation temperature and shortens the start and duration of local transformation.

Figure 10 shows the influence of increasing diameter on the surface and center temperature/transformation. In the larger diameter rods the time to start, and the duration of the transformation, is greater. As a result of the thermal arrest, the transformation is nearly isothermal, particularly in the larger rods. Also it is seen that transformation in the center of the 5.5 mm rod lags only two seconds behind the surface, whereas in the 25 mm rod, the surface transformation is virtually complete before transformation at the center commences. As expected, the transformation temperature at the surface is significantly lower than that at the center in the 25 mm rod as compared to the 5.5 mm rod; thus the

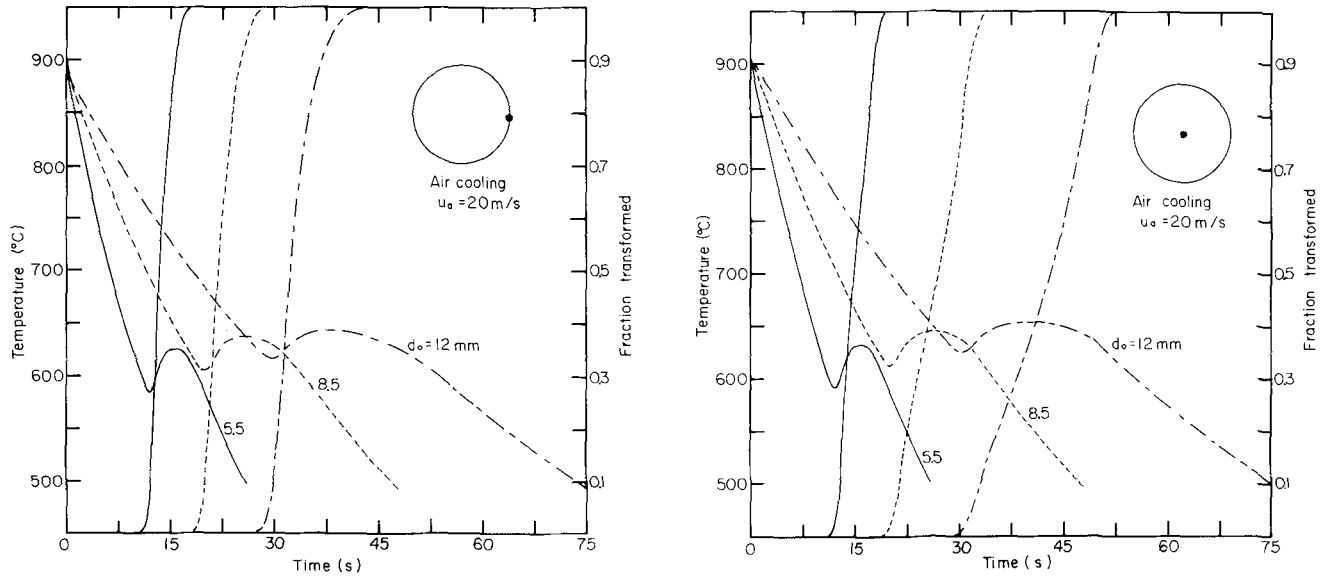

Fig. 14—Effect of rod diameter on the local temperature and fraction austenite transformed at the surface and center of rods with air cooling at 20 m/s.

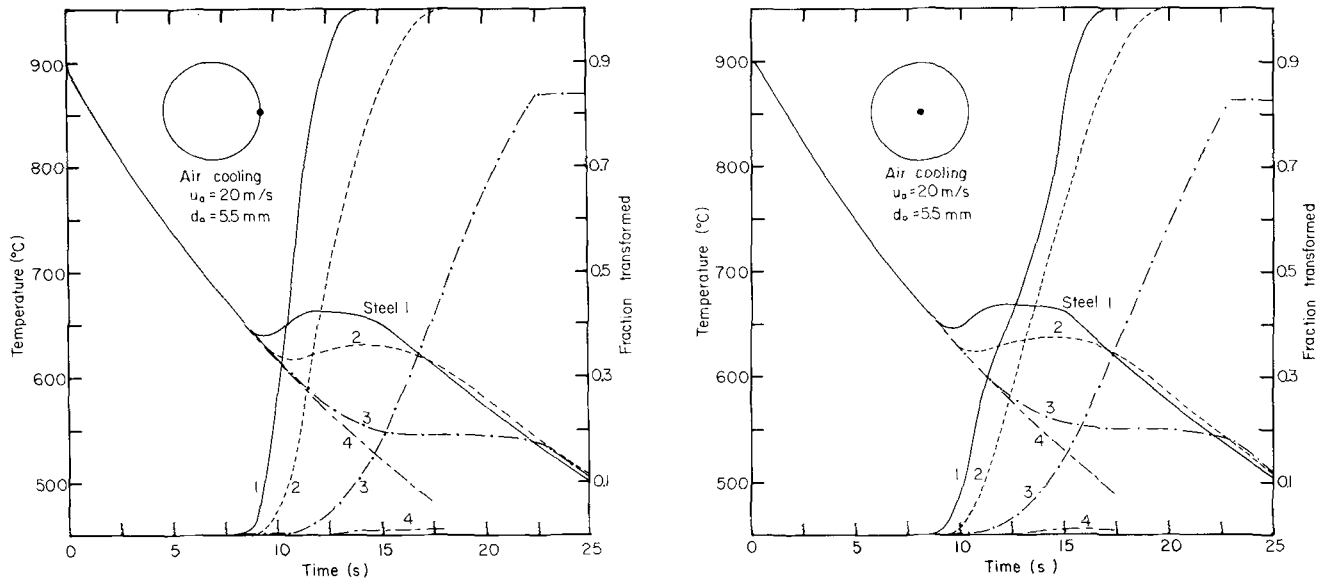

Fig. 15—Effect of pct Mn and grain size of steel on the local temperature and fraction austenite transformed at the surface and center of a 5.5 mm diam rod with air cooling at 20 m/s.

pearlite spacing in the former may increase considerably from the surface to the center.

The effect of varying pct Mn in the steel was investigated using *T-T-T* diagrams presented in Fig. 11, while the temperature and transformation predictions, in the absence of ferrite formation, are shown in Fig. 12. Thus it is observed that with increasing pct Mn, the duration of the transformation is increased particularly at the surface of the rod. Indeed in the cases of steels 3 and 4 the transformation is not fully completed, with the latter consisting almost entirely of bainite and martensite. This is not surprising since Mn has the effect of pushing the *C*-curves on the *T-T-T* diagram to longer times. Note also that for these cooling conditions, pct Mn has a strong effect on the transformation temperature and hence pearlite structure.

b. Air Cooling

The air cooling of steel rods has been simulated using radiation theory and standard correlations for the cross flow of air over a cylinder to characterize h in Eq. [3]. For the special case of no air flow, natural convection correlations have been employed. The calculations have been performed mainly for 5.5 mm diam rods and an air velocity of 20 m/s. Figure 13 shows the influence of air velocity over the range of 0 to 40 m/s. The largest effect is seen between 0 and 10 m/s in which the transformation start and end on the rod surface are decreased about two-fold, and the transformation temperature is reduced by roughly 25 °C. Further increases in air velocity reduce the transformation temperature by another 20 °C giving rise to finer pearlite.

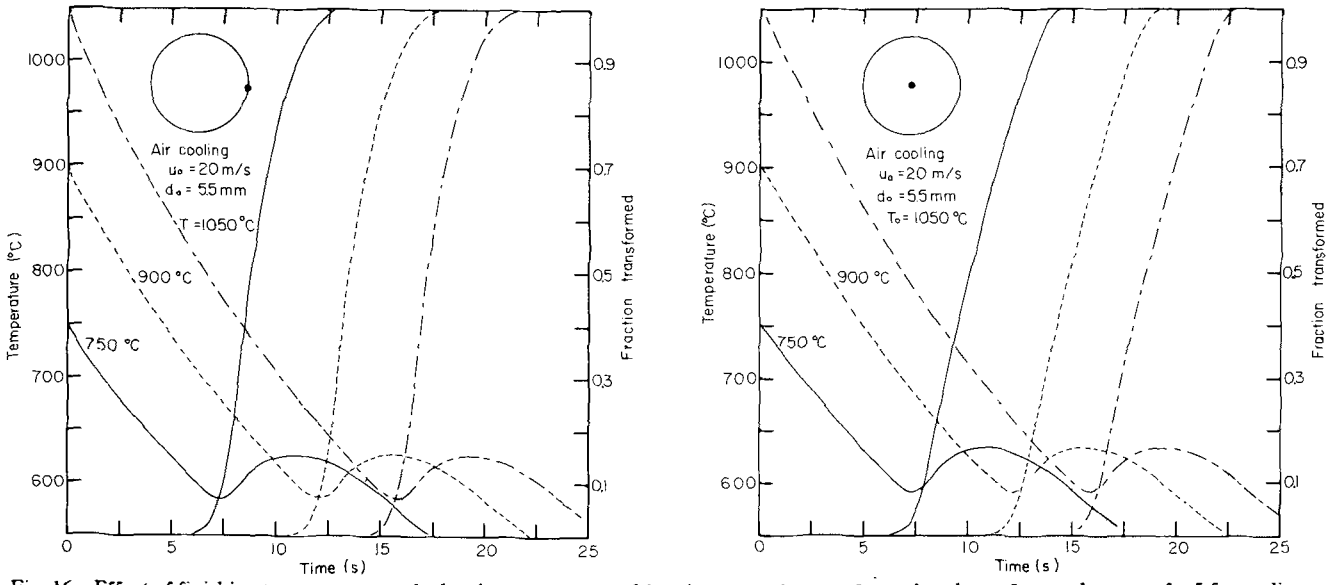

Fig. 16—Effect of finishing temperature on the local temperature and fraction austenite transformed at the surface and center of a 5.5 mm diam rod with air cooling at 20 m/s.

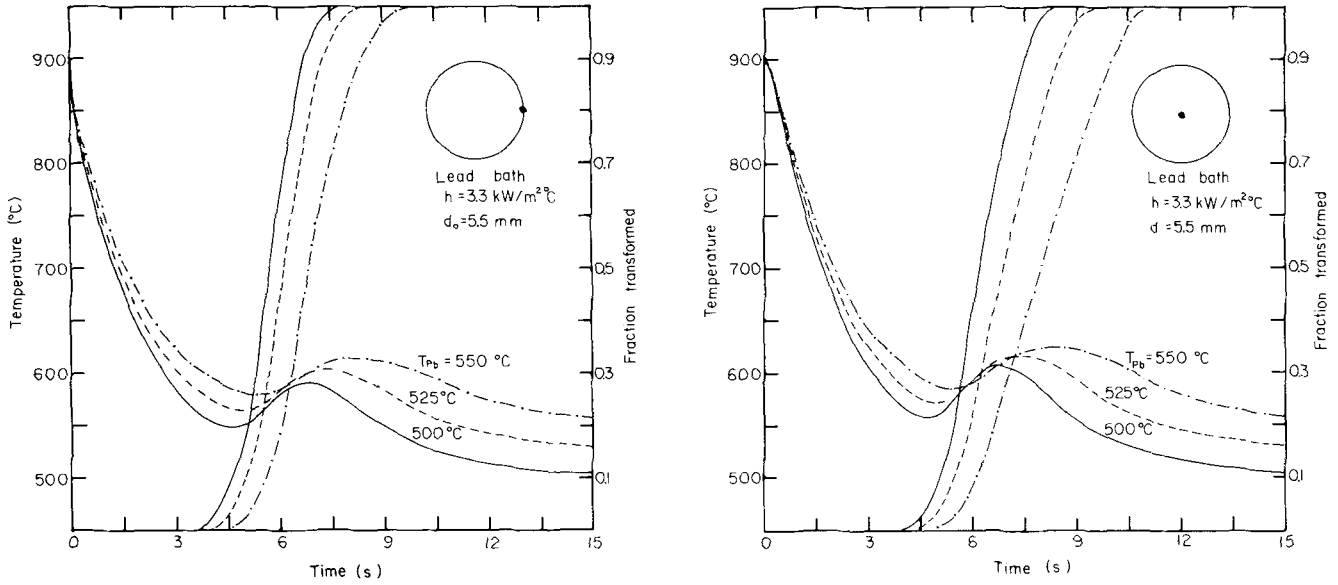

Fig. 17—Effect of lead bath temperature on the local temperature and fraction austenite transformed at the surface and center of a 5.5 mm diam rod.

Figure 14 shows the effect of diameter on the local temperature/transformation at the surface and center of the rods. The effect is large similar to that seen under quench conditions, Fig. 10. A two-fold increase in diameter increases the time to start and complete transformation at the rod surface by roughly 2.5; the effect is larger at the center.

Figures 15 and 16 show the influence of pct Mn and finishing temperature respectively under air cooling conditions. The Mn content of the steel affects the temperature and transformation in much the same way as observed in Fig. 12 for quench conditions. Changing the finishing temperature simply translates the cooling/transformation curves to longer or shorter times, but does not alter the transformation temperature. Thus, for constant cooling conditions, the pearlite structure should be unaffected by finishing temperature.

c. Lead Bath

The effect of lead-bath temperature is presented in Fig. 17 for a 5.5 mm diam rod. Increasing the bath temperature increases the transformation temperature proportionally and results in a coarser pearlite. On a practical note, with bath temperatures much below 500 °C bainite may form.

5. INDUSTRIAL APPLICATIONS

The predictions shown here demonstrate the potential usefulness of the model in designing, and solving problems in metal cooling systems like quenching, Stelmor cooling or lead patenting. From the design standpoint, the model can be employed to predict the cooling requirements of a given rod size and eutectoid

steel composition to achieve a desired structure which is a function of the transformation temperature. For a Stelmor line, for example, predictions of cooling time and air velocity in each zone is possible. With regard to solving problems such as center segregation of C or Mn, the model can be used to predict the cooling conditions necessary to avoid the formation of martensite. However, the accuracy of the predictions depends critically on the availability of reliable *T-T-T* diagrams. These subjects are taken up in a paper to follow.

6. SUMMARY

A mathematical model has been developed to predict the coupled heat flow and austenite-pearlite transformation during the cooling of eutectoid carbon steel rods. The model predictions have been checked under simplified conditions by comparison to analytical solutions of temperature and fraction austenite transformed. A comparison has also been made between model predictions and measurements of the center temperature in rods of different sizes. The model has been used to study the influence of important process variables on the transformation behavior of rods under conditions of quench-, air- and lead-cooling.

APPENDIX I

Prediction of Transformation "Start" During Continuous Cooling Using Two Parameter Equation

Referring to Fig. 3, the cooling curve is subdivided into a series of small time intervals each of which is isothermal. From Eq. [5] the fraction of austenite transformed in the first time interval below the AC_1 temperature is

$$F_1 = 1 - \exp\left[-C(T_1)\Delta t_1^{n(T_1)}\right] \quad [A1]$$

where

$$C(T_1) = \frac{1}{\alpha_1^{n(T_1)}} \ln\left[\frac{1}{1 - F_s}\right] \quad [A2]$$

Then following the procedure outlined in the text the fraction transformed by the end of the second time step with temperature T_2 is

$$F_2 = 1 - \exp\left[-C(T_2)\theta_2^{n(T_2)}\right] \quad [A3]$$

where according to Eq. [7] θ_2 is the sum of the second time interval and the time required to achieve F_1 at T_2

$$\theta_2 = \Delta t_2 + \left[\frac{\ln\left(\frac{1}{1 - F_1}\right)}{C(T_2)}\right]^{1/n(T_2)} \quad [A4]$$

Substituting Eqs. [A1] and [A4] into Eq. [A3] and taking advantage of the relationship

$$C(T_1)\alpha_1^{n(T_1)} = C(T_2)\alpha_2^{n(T_2)} \quad [A5]$$

one obtains for F_2

$$F_2 = 1 - \exp\left[-C(T_2)\alpha_2^{n(T_2)} \times \left\{\left(\frac{\Delta t_1}{\alpha_1}\right)^{n(T_1)/n(T_2)} + \left(\frac{\Delta t_2}{\alpha_2}\right)\right\}^{n(T_2)}\right] \quad [A6]$$

And for the m^{th} time interval

$$F_m = 1 - \exp\left\{-C(T_m)\alpha_m^{n(T_m)} \times \left[\left[\ldots\left[\left[\left(\frac{\Delta t_1}{\alpha_1}\right)^{n(T_1)/n(T_2)} + \frac{\Delta t_2}{\alpha_2}\right]^{n(T_2)/n(T_3)} + \frac{\Delta t_3}{\alpha_3}\right]^{n(T_3)/n(T_4)} + \ldots + \frac{\Delta t_{m-1}}{\alpha_{m-1}}\right]^{n(T_{m-1})/n(T_m)} + \frac{\Delta t_m}{\alpha_m}\right]^{n(T_m)}\right\} \quad [A7]$$

Also it is seen that

$$C(T_m) \cdot \alpha_m^{n(T_m)} = \ln\left(\frac{1}{1 - F_s}\right) \quad [A8]$$

and after substituting into Eq. [A7] and rearranging

$$\left[\frac{\ln(1 - F_m)}{\ln(1 - F_s)}\right]^{1/n(T_m)} = \left[\left[\ldots\left[\left[\left(\frac{\Delta t_1}{\alpha_1}\right)^{n(T_1)/n(T_2)} + \frac{\Delta t_2}{\alpha_2}\right]^{n(T_2)/n(T_3)} + \frac{\Delta t_3}{\alpha_3}\right]^{n(T_3)/n(T_4)} + \ldots + \frac{\Delta t_{m-1}}{\alpha_{m-1}}\right]^{n(T_{m-1})/n(T_m)} + \frac{\Delta t_m}{\alpha_m}\right] \quad [A9]$$

If n is constant and m is such that the transformation start line is reached during the m^{th} step, *i.e.* $F_m = F_s$, then

$$\sum_{j=1}^{m} \frac{\Delta t_j}{\alpha_j} = 1 \quad [A10]$$

which is the Scheil Equation.

APPENDIX II

Analytical Expression for Fraction of Austenite Transformed at Constant Cooling Rate

It was desirable to obtain an analytical solution for the fraction of austenite transformed in order to test the transformation section of the model for internal consistency. Thus, assuming n to be constant, the fraction of austenite transformed at the end of the m^{th} time step according to Eq. [A9] is

$$\left[\frac{\ln(1 - F_m)^{1/n}}{\ln(1 - F_s)}\right] = \sum_{j=1}^{m} \frac{\Delta t}{\alpha_j} \quad [A11]$$

and at the end of the $(m + 1)^{th}$ step

$$\left[\frac{\ln(1 - F_{m+1})}{\ln(1 - F_s)}\right]^{1/n} = \sum_{j=1}^{m+1} \frac{\Delta t}{\alpha_j} \quad [A12]$$

Subtracting Eq. [A11] from Eq. [A12], the RHS becomes $\Delta t/\alpha_{m+1}$; and after dividing by Δt, and taking the limit $\Delta t \to 0$, one obtains

$$\frac{d}{dt}\left[\left\{\frac{\ln(1-F)}{\ln(1-F_s)}\right\}^{1/n}\right] = \frac{1}{\alpha} \qquad [A13]$$

This is the basic differential equation for the transformation which can be solved by characterizing α as a function of time t from the cooling conditions and the equation for the *T-T-T* curve. For example, referring to Fig. 3, the transformation start line is once again approximated by a series of line segments.

$$T = A_k \ln \alpha + B_k \qquad [A14]$$

In addition, to simplify matters, the cooling rate R is assumed to be constant

$$T = T_{AC_1} - R(t - t_{AC_1}) \qquad [A15]$$

Thus, at a given temperature, T, α can be related to the cooling time, $t\,(= j \cdot \Delta t)$, as follows

$$\frac{1}{\alpha} = \exp\left[\frac{B_k - T_{AC_1} + R(t - t_{AC_1})}{A_k}\right] \qquad [A16]$$

$$d\left(\frac{1}{\alpha}\right) = \frac{R}{A_k} \cdot \frac{1}{\alpha} \cdot dt$$

$$\frac{1}{\alpha}\,dt = \frac{A_k}{R} \cdot d\frac{1}{\alpha} \qquad [A17]$$

substituting Eq. [A17] in Eq. [A13] and integrating between the line segments of the *T-T-T* curve the following equation is obtained

$$\left[\frac{\ln(1-F)}{\ln(1-F_s)}\right]^{1/n} = \frac{A_1}{R}\int_{\alpha_0^*}^{\alpha_1^*} d\,\frac{1}{\alpha} + \frac{A_2}{R}\int_{\alpha_1^*}^{\alpha_2^*} d\,\frac{1}{\alpha} + \ldots + \frac{A_{l-1}}{R}\int_{\alpha_{l-2}^*}^{\alpha_{l-1}^*} d\,\frac{1}{\alpha} + \frac{A_l}{R}\int_{\alpha_{l-1}^*}^{\alpha} d\,\frac{1}{\alpha}$$

$$= \sum_{k=1}^{l-1}\frac{A_k}{R}\left[\frac{1}{\alpha_k^*} - \frac{1}{\alpha_{k-1}^*}\right] + \frac{A_l}{R}\left[\frac{1}{\alpha} - \frac{1}{\alpha_{l-1}^*}\right] \qquad [A18]$$

where $\alpha_{l-1}^* < \alpha < \alpha_l^*$. The value of α can be obtained from Eq. [A16].

NOMENCLATURE

A slope of line segment for F_s C-curve.
B temperature intercept of line segment for F_s C-curve.
C parameter in Eq. [5].
C_p specific heat (kJ/kg °C).
D slope of line segment for F_f C-curve.
E temperature intercept of line segment for F_f C-curve.
F fraction of austenite transformed to pearlite.
ΔF incremental fraction of austenite transformed to pearlite in time interval Δt.
F_s fraction pearlite at transformation start.
F_f fraction pearlite at transformation end.
G growth rate of pearlite nucleii (m/s).
H heat of transformation (J/kg).
h heat transfer coefficient (kW/m² °C).
k thermal conductivity (kW/m °C).
N_v rate of nucleation (1/m³s).
n parameter in Eq. [5].
$\dot{q}$ volumetric rate of heat generation (kW/m³).
R cooling rate (°C/s).
r radial position in the rod (m).
r_o radius of the rod (m).
Δr increment of radius (m).
T temperature (°C).
T_{AC_1} temperature of AC_1 line (°C).
t time on cooling curve (s).
t_{AC_1} cooling time to reach T_{AC_1}.
Δt increment of time (s).

Greek Letters
α isothermal transformation time to transform fraction F_s.
β isothermal transformation time to transform fraction F_f.
ρ density (kg/m³).
θ virtual time defined by Eq. [7].

Superscripts
$*$ bounding values of line segments of *T-T-T* curves.
i node position.

Subscripts
AC_1 AC_1 line.
AP austenite to pearlite transformation.
a ambient.
f end of transformation.
in initial.
j index of time increment.
k index of line segments of *T-T-T* curves.
r_o surface.
s start of transformation.

ACKNOWLEDGMENTS

The authors are grateful to the Dept. of Metallurgical Engineering, U.B.C. for support of this work, part of which was completed to fulfill course requirements for the M.A.Sc. degree. Thanks are also extended to Dr. E. B. Hawbolt and Mr. B. Prabhakar who assisted in the study.

REFERENCES

1. *Physical Constants of Some Commercial Steels at Elevated Temperatures*, BISRA, Scientific Publications, London, 1978.
2. J. K. Kramer, G. M. Pound, and R. F. Mehl: *Acta Metall.*, 1958, vol. 6, pp. 653–71.
3. F. Kreith: *Principles of Heat Transfer*, 3rd ed., Intext Publishers, New York, 1973.
4. D. Sieurin and A. A. Jalil: *The Versatile Stelmor Process—Three Systems for Controlled Cooling of Wire Rod*, Morgan, Worcester.
5. W. A. Johnson and R. F. Mehl: *Trans. AIME*, 1939, vol. 135, pp. 416–58.

6. *Atlas of Isothermal Transformation and Cooling Transformation Diagrams*, ASM, Metals Park, OH, 1977.
7. *Atlas of Isothermal Transformation Diagrams*, U.S. Steel, 1961.
8. E. Scheil: *Arch. Eisenhuttenw.*, 1935, vol. 12, pp. 565–67.
9. W. L. Bradley and R. Mattos: *Data Mater. Sci. Eng.*, 1975, vol. 21, pp. 227–37.
10. N. Shimizu, and I. Tamura: *Trans. Iron Steel Inst. Jpn.*, 1977, vol. 17, pp. 469–76.
11. B. Carnahan, H. A. Luther, and J. O. Wilkes: *Applied Numerical Methods*, John Wiley, 1969, pp. 441–46.
12. G. E. Myers: *Analytical Methods in Conduction Heat Transfer*, McGraw-Hill, 1971.
13. K. Takeo, K. Maeda, T. Kamise, H. Iwata, Y. Satomi, and M. Nakata: *Trans. Iron Steel Inst. Jpn.*, 1975, vol. 15, pp. 422–28.